Draft version July 6, 2022
Typeset using LaTeX **twocolumn** style in AASTeX631

Speckle Interferometry at SOAR in 2021

Andrei Tokovinin,[1] Brian D. Mason,[2] Rene A. Mendez,[3] and Edgardo Costa[3]

[1] *Cerro Tololo Inter-American Observatory — NFSs NOIRLab Casilla 603, La Serena, Chile*
[2] *U.S. Naval Observatory, 3450 Massachusetts Ave., Washington, DC, USA*
[3] *Universidad de Chile, Casilla 36-D, Santiago, Chile*

ABSTRACT

The speckle interferometry program at the the 4.1 m Southern Astrophysical Research Telescope (SOAR), started in 2008, now accumulated over 30,300 individual observations of 12,700 distinct targets. Its main goal is to monitor orbital motion of close binaries, including members of high-order hierarchies and low-mass dwarfs in the solar neighborhood. The results from 2021 are published here, totaling 2,623 measurements of 2,123 resolved pairs and non-resolutions of 763 targets. The median measured separation is 0.″21, and 75 pairs were closer than 30 mas. The calibration of scale and orientation is based on the observations of 103 wide pairs with well-modeled motion. These calibrators are compared to the latest Gaia data release, and minor (0.5%) systematic errors were rectified, resulting in accurate relative positions with typical errors on the order of 1 mas. Using these new measurements, orbits of 282 binaries are determined here (54 first determinations and 228 corrections). We resolved for the first time 50 new pairs, including subsystems in known binaries. A list of 94 likely spurious pairs unresolved at SOAR (mostly close Hipparcos binaries) is also given.

Keywords: Visual Binary Stars; Orbital Elements; Multiple Stars

1. INTRODUCTION

This paper continues the series of double-star measurements made at the 4.1 m Southern Astrophysical Research Telescope (SOAR) since 2008 with the speckle camera, HRCam. Previous results were published by Tokovinin, Mason, & Hartkopf (2010a, hereafter TMH10) and in (Tokovinin et al. 2010b; Hartkopf et al. 2012; Tokovinin 2012; Tokovinin et al. 2014, 2015, 2016, 2018a, 2019, 2020, 2021). Observations reported here were made during 2021.

The structure and content of this paper are similar to other paper of this series. Section 2 reviews all speckle programs that contributed to this paper, the observing procedure, and the data reduction. The results are presented in Section 3 in the form of electronic tables archived by the journal. We also discuss new resolutions, present new orbits resulting from this data set, and give a list of likely spurious unresolved pairs. A short summary and an outlook of further work in Section 4 close the paper.

andrei.tokovinin@noirlab.edu

brian.d.mason.civ@us.navy.mil

rmendez@uchile.cl

2. OBSERVATIONS

2.1. *Observing Programs*

As in previous years, HRCam (see Section 2.2) was used during 2021 to execute several observing programs, some with common targets. Table 1 gives an overview of these programs and indicates which observations are published in the present paper. The numbers of observations are approximate. Overall, 5,138 observations were made during 2021. Here is a brief description of the main programs.

Orbits of resolved binaries. New measurements contribute to the steady improvement of the quantity and quality of orbits in the Sixth Catalog of Visual Binary Star Orbits (Hartkopf, Mason & Worley 2001). See Anguita-Aguero et al. (2022); Gómez et al. (2022) as recent examples of this work. We provide a large table of updated and first-time orbits in Section 3.3.

Table 1. Observing programs

Program	PI	N	Publ.[a]
Orbits	Mason, Tokovinin	1092	Yes
Hierarchical systems	Tokovinin	149	Yes
Hipparcos binaries	Mendez, Horch	451	Yes
Neglected binaries	R. Gould, Mason	624	Yes
Nearby M dwarfs	E. Vrijmoet	323	No
TESS follow-up	C. Ziegler	724	No
Acceleration stars	K. Franson	388	No

[a] This columns indicates whether the results are published here (Yes) or deferred to future papers (No).

Hierarchical systems of stars are of special interest because their architecture is relevant to star formation, while dynamical evolution of these hierarchies increases chances of stellar interactions and mergers (Tokovinin 2021b). Orbital motions of several triple systems are monitored at SOAR and these data are used for the orbit determinations (Tokovinin & Latham 2020; Tokovinin 2021a).

Hipparcos binaries within 200 pc are monitored to measure masses of stars and to test stellar evolutionary models, as outlined by, e.g., Horch et al. (2015, 2017, 2019). The southern part of this sample is addressed at SOAR (Mendez et al. 2017). This program overlaps with the general work on visual orbits.

Neglected close binaries from the Washington Double Star Catalog, WDS (Mason et al. 2001),[1] were observed as a 'filler' at low priority. In some cases, we resolved new inner subsystems, thus converting classical visual pairs into hierarchical triples. Some WDS pairs are moving fast near periastron, allowing calculation of their first orbits after several observations at SOAR. Another result of this effort is a list of spurious pairs that should be removed from the WDS.

Nearby K and M dwarfs are being observed at SOAR since 2018 following the initiative of T. Henry and E. Vrijmoet. The goal is to assemble statistical data on orbital elements, focusing on short periods. The sample includes known and suspected binaries detected by astrometric monitoring, Gaia, etc. First results on M dwarfs are published by Vrijmoet et al. (2022). In 2021, we continued to monitor these pairs, some of them with fast orbital motion.

TESS follow-up continues the program executed in 2018–2020. Its results are published in (Ziegler et al. 2020, 2021). All speckle observations of TESS targets of interest are promptly posted on the EXOFOP web site. These data are used in the growing number of papers on TESS exoplanets, mostly as limits on close companions to exohosts.

Accelerating stars were observed as potential targets of high-contrast imaging of exoplanets in a program led by K. Franson and B. Bowler. A substantial fraction of nearby stars with small accelerations, detected by comparing Gaia and Hipparcos astrometry (Brandt 2021), are just binaries with stellar companions. Their resolution at SOAR serves to clean the target list for high-contrast imaging of the remaining stars (possible exohosts) and presents an independent interest for future orbit calculation and multiplicity statistics.

Observations of young stars belonging to moving groups were published in our previous paper (Tokovinin et al. 2021). In 2021, a modest number of additional targets from this program were observed.

If observations of a given star were requested by several programs, they are published here even when the other program still continues. We also publish here the measurements of previously known pairs resolved during surveys, for example in the TESS follow-up.

The observations were grouped into 12 observing runs lasting from 0.5 to 3 nights each. The time allocated in 2021 through NOIRLab and Chilean TACs amounted to 10 nights, two more nights were contributed by the SOAR partners for TESS follow-up, and some engineering time (morning hours of 8 nights equivalent to 3 full nights) was also used for speckle observations.

2.2. *Instrument and Observing Procedure*

The observations reported here were obtained with the *high-resolution camera* (HRCam) — a fast imager designed to work at the 4.1 m SOAR telescope (Tokovinin 2018). The instrument and observing procedure are described in the previous papers of these series (e.g. Tokovinin et al. 2020), so only the basic facts are reminded here. HRCam receives light through the SOAR Adaptive Module (SAM) which provides correction of the atmospheric dispersion. We used mostly the near-infrared I filter (824/170 nm) and the Strömgren y filter (543/22 nm), with four observations made in the V filter; the transmission curves of HRCam filters are given in the instrument manual. In the standard observing mode, two series of 400 200×200 pixel images (image cubes) are recorded. The pixel scale is 0.″01575, so the field of view is 3.″15; the exposure time is normally 24 ms. For survey programs such as TESS follow-up, we use the I filter and a 2×2 binning, doubling the field. Pairs wider than ∼1.″4 are observed with a 400×400 pixel field, and

[1] See the latest online WDS version.

the widest pairs are sometimes recorded with the full field of 1024 pixels (16″) and a 2×2 binning.

The speckle power spectra are calculated and displayed immediately after acquisition for quick evaluation of the results. Observations of close pairs are accompanied by observations of single (reference) stars to account for such instrumental effects as telescope vibration or aberrations. Bright stars can be resolved and measured below the formal diffraction limit by fitting a model to the power spectrum and using the reference. The resolution and contrast limits of HRCam are further discussed in TMH10 and in the previous papers of this series. The standard magnitude limit is $I \approx 12$ mag under typical seeing; pairs as faint as $I \approx 16$ mag were measured under exceptionally good seeing, albeit with reduced accuracy and resolution.

Custom software helps to optimize observations by selecting targets, pointing the telescope, and logging. Typically, about 300 targets are covered on a clear night. The observing programs are executed in an optimized way, depending on the target visibility, atmospheric conditions, and priorities, while minimizing the telescope slews. Reference stars and calibrator binaries are observed alongside the main targets as needed; their observations are published here as well.

2.3. *Data Processing*

The data processing is described in TMH10 and Tokovinin (2018). We use the standard speckle interferometry technique based on the calculation of the power spectrum and the speckle autocorrelation function (ACF). Companions are detected as secondary peaks in the ACF and/or as fringes in the power spectrum. Parameters of the binary and triple stars (separation ρ, position angle θ, and magnitude difference Δm) are determined by modeling (fitting) the observed power spectrum. The true quadrant is found from the shift-and-add (SAA) images whenever possible because the standard speckle interferometry determines position angles modulo 180°. The resolution and detection limits are estimated for each observation.

2.4. *Calibration of Scale and Orientation*

Since 2014, the pixel scale and angular offset of HRCam are inferred from observations of several relatively wide (from 0.″5 to 3″) calibration binaries, called *calibrators* for brevity. Their motion is accurately modeled based on previous observations at SOAR (Tokovinin et al. 2015). Before 2014, the HRCam calibration was derived from special experiments described in TMH10 and from the comparison of HRCam with the wide-field imager, SAMI, attached to another port of SAM. The scale and orientation of both imagers were mutually related by mapping the motion of a point source located at the SAM focal plane and mounted on the translation stages. The orientation of SAMI was determined from the astrometric solutions of sky images.

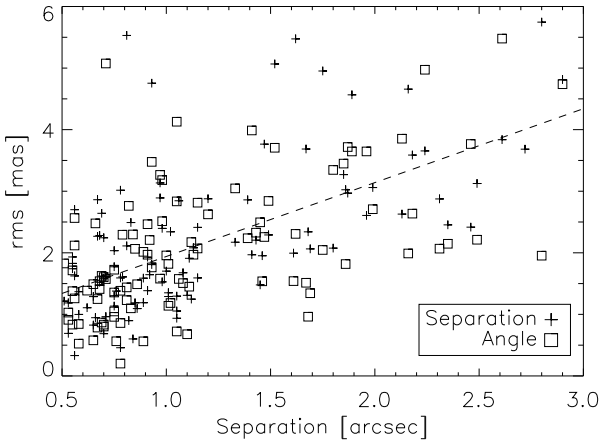

Figure 1. Dependence of the rms residuals of calibrators on the separation. Plus signs and squares correspond to radial $\Delta\rho$ and tangential $\rho\Delta\theta$ residuals, respectively, and the dashed line is a linear fit to both.

We revised here the list of calibrators and their models using all SOAR observations from 2007.7 to 2021.75. After removing faint stars and binaries with known or suspected subsystems, the list counts 103 calibrators. The motion of 88 calibrators is modeled by their visual orbits, specially adjusted to accurately represent the HRCam measurements (many of those orbits are of low grade owing to the insufficient coverage); the remaining 15 pairs are modeled by linear functions of the separation ρ and position angle θ vs. time.

Using the new models of the calibrators, small corrections of the angular offset and scale for each observing run were recomputed and applied. Figure 1 plots the rms residuals σ between observations and models in the radial and tangential directions vs. separation ρ. The residuals in both directions are similar, and they can be jointly approximated by the linear formula

$$\sigma \approx 0.81 + 1.15\rho \quad \text{mas}. \tag{1}$$

Thus, a 1″ binary is measured by HRCam with a typical accuracy of 2 mas. A linear increase of measurement errors with separation is expected from the physics of light propagation through the atmosphere (differential tilts). Equation 18 from Kenyon et al. (2006) with parameters $C_1 = 500\,\text{arcsec}\,\text{rad}^{-1}\ \text{m}^{2/3}\,\text{s}^{1/2}$, typical for Cerro Pachón, binary separation of 1″, exposure time of 8 s, and baseline of 2 m (half telescope diameter) predicts the atmospheric error of 0.5 mas, less than 2 mas according to (1) and roughly matching the lower envelope of

points in Figure 1. Note, however, that the calibrator's model errors and the residual calibration errors of individual runs also contribute to σ and these contributions increase linearly with ρ. Calibrators with a large Δm have larger residuals to models.

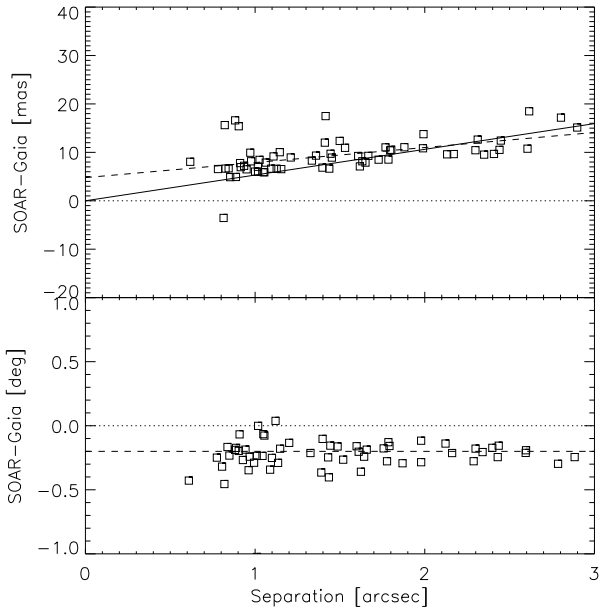

Figure 2. Dependence of the difference between SOAR and Gaia positions in separation (top) and angle (bottom) on the separation. In the top plot, the dashed line is a linear fit and the solid line is a scale factor.

The set of calibrators assures a good consistency between the observing runs, but might contain small global offsets in angle and scale, being based entirely on the HRCam data. An external comparison is needed to control the systematics. Here we compare the updated calibrator models with the relative positions of these pairs derived from the Gaia Early Data Release 3 (EDR3) astrometry (Gaia collaboration 2021) and referring to the nominal epoch 2016.0. For some closer pairs, the Gaia positions strongly deviate from the 2016.0 positions inferred from the models, suggesting errors in the Gaia reductions. In most such pairs with bad or suspicious Gaia positons, there are no parallaxes and proper motions (PMs) for one or both components. The remaining 58 pairs demonstrate good consistency between Gaia positions and models, allowing us to look for systematic differences.

The comparison between the good Gaia EDR3 calibrators and their models is shown in Figure 2. A simple linear fit to the separation differences gives

$$\rho_{\rm SOAR} - \rho_{\rm EDR3} \approx 4.8 + 3.11\rho \quad \text{mas}, \qquad (2)$$

as shown by the dashed line in the top plot. The existence of an offset at zero separation is not expected; it could result from the errors of the fit. If real, this is probably an artifact of the Gaia measurement algorithm related to blended sources (a similar offset was found in the Gaia DR2 positions). If only the 26 calibrators wider that 1.″5 are selected, the mean scale factor is $\rho_{\rm SOAR}/\rho_{\rm EDR3} = 1.0053$, and its rms scatter is 0.0009. The formal error of the mean scale factor is thus 10^{-4}. The bottom panel of Figure 2 clearly shows an offset between the position angles of Gaia EDR3 and SOAR. The mean offset is $\theta_{\rm SOAR} - \theta_{\rm EDR3} = -0.^\circ21$, the rms scatter is $0.^\circ095$, and the formal error of the mean is $0.^\circ02$.

In the light of the comparison of calibrators with Gaia, the separations measured by HRCam so far must be divided by the scale factor of 1.0053 (decrease by half a percent), and all position angles must be increased by $0.^\circ2$. These corrections have a negligibly small effect on the orbits of close binaries derived from our data, but are relevant when a small wobble in the motion of wide pairs is studied and when the HRCam data are used jointly with the Gaia relative positions. These corrections are applied to the models of the calibrators and to the measurements published here.

Our strategy of observing wide pairs with slow motion for retroactive calibration, adopted from the beginning of the SOAR speckle program, has proven to be correct. Although the orbits of most such binaries are not of high quality, they can accurately represent the observed motion and serve for comparison with Gaia. The alternative strategy of using good-quality orbits of fast and close pairs, adopted by some other speckle programs (e.g. Horch et al. 2021), delivers a substantially inferior calibration precision. For example, a 100 mas pair measured with a 1 mas accuracy cannot constrain the calibration to better than 1%, even if its orbit were known exactly.

3. RESULTS

3.1. *Data Tables*

The results (measures of resolved pairs and non-resolutions) are presented in exactly the same format as in Tokovinin et al. (2021). The long tables are published in machine-readable format; here we describe their content.

Table 2 lists 2,623 measures of 2,123 resolved pairs and subsystems, including new discoveries. The pairs are identified by their WDS-style codes based on the

Table 2. Measurements of Double Stars at SOAR

Col.	Label	Format	Description, units
1	WDS	A10	WDS code (J2000)
2	Discov.	A16	Discoverer code
3	Other	A12	Alternative name
4	R.A.	F8.4	R.A. J2000 (deg)
5	Decl.	F8.4	Declination J2000 (deg)
6	Epoch	F9.4	Julian year (yr)
7	Filt.	A2	Filter
8	N	I2	Number of averaged cubes
9	θ	F8.1	Position angle (deg)
10	$\rho\sigma_\theta$	F5.1	Tangential error (mas)
11	ρ	F8.4	Separation (arcsec)
12	σ_ρ	F5.1	Radial error (mas)
13	Δm	F7.1	Magnitude difference (mag)
14	Flag	A1	Flag of magnitude difference[a]
15	$(O-C)_\theta$	F8.1	Residual in angle (deg)
16	$(O-C)_\rho$	F8.3	Residual in separation (arcsec)
17	Ref	A9	Orbit reference[b]

[a] Flags: q – the quadrant is determined; * – Δm and quadrant from average image; : – noisy data or tentative measures.

[b] References are provided at https://www.astro.gsu.edu/wds/orb6/wdsref.txt

Table 3. Unresolved Stars

Col.	Label	Format	Description, units
1	WDS	A10	WDS code (J2000)
2	Discov.	A16	Discoverer code
3	Other	A12	Alternative name
4	R.A.	F8.4	R.A. J2000 (deg)
5	Decl.	F8.4	Declination J2000 (deg)
6	Epoch	F9.4	Julian year (yr)
7	Filt.	A2	Filter
8	N	I2	Number of averaged cubes
9	$\rho_{\min}$	F7.3	Angular resolution (arcsec)
10	$\Delta m(0.15)$	F7.2	Max. Δm at $0''.15$ (mag)
11	$\Delta m(1)$	F7.2	Max. Δm at $1''$(mag)
12	Flag	A1	: marks noisy data

J2000 coordinates and discoverer designations adopted in the WDS catalog (Mason et al. 2001), as well as by alternative names in column (3), mostly from the Hipparcos catalog. Equatorial coordinates for the epoch J2000 in degrees are given in columns (4) and (5) to facilitate matching with other catalogs and databases. In the case of resolved multiple systems, the position measurements and their errors (columns 9–12) and magnitude differences (column 13) refer to the individual pairings between components, not to their photocenters. As in the previous papers of this series, we list the internal errors derived from the power spectrum model and from the difference between the measures obtained from two data cubes. The real errors are usually larger, especially for difficult pairs with substantial Δm and/or with small separations. Residuals from orbits and from the models of calibrators, typically between 1 and 5 mas rms, characterize the external errors of the HRcam astrometry (Figure 1).

The flags in column (14) indicate the cases where the true quadrant is determined (otherwise the position angle is measured modulo 180°), when the relative photometry of wide pairs is derived from the long-exposure images (this reduces the bias caused by speckle anisoplanatism), and when the data are noisy or the resolutions are tentative (see TMH10). For binary stars with known orbits, the residuals to the latest orbit and its reference are provided in columns (15)–(17). Residuals close to 180° mean that the orbit swaps the brighter (A) and fainter (B) stars. However, in some binaries the secondary is fainter in one filter and brighter in other (e.g. 15234−5919). In these cases, it is better to keep the historical identification of the components in agreement with the orbit and to give a negative magnitude difference Δm.

Nonresolutions are reported in Table 3. Its first columns (1) to (8) have the same meaning and format as in Table 2. Column (9) gives the minimum resolvable separation when pairs with $\Delta m < 1$ mag are detectable. It is computed from the maximum spatial frequency of the useful signal in the power spectrum and is normally close to the formal diffraction limit λ/D. The following columns (10) and (11) provide the indicative dynamic range, i.e. the maximum magnitude difference at separations of $0''.15$ and $1''$, respectively, at 5σ detection level. The last column (12) marks noisy data by the flag ":". In Table 4 we provide short notes on some pairs, mostly the alternative designations and relevant references.

3.2. *New Pairs*

Table 5. New Double Stars

WDS J2000	Name	ρ (arcsec)	Δm (mag)	Program[a]
00272−7324	TOK 908	0.24	1.7	HIP
00438−3911	TOK 909	0.66	3.6	HIP
01333−5142	TOK 910	0.36	2.6	HIP
02035−3005	RST 2270 Aa,Ab	0.22	3.1	MSC
03230−7047	HEI 630 BC	0.12	0.8	MSC
03385+1336	YR 10 Ab1,Ab2	0.04	0.7	MSC[b]
05053−4208	BRT 668 Aa,Ab	0.15	2.2	TESS

Table 5 *continued*

Table 4. Notes

WDS	Comment
02346−4210	This is WDSS 0234367−421019 (HIP 11989), see 2020ApJS..247...66H
02434−6643	B is fainter than A in y filter, but brighter in I.
02415−7128	HIP 12548 is a quadruple system, orbits in 2022AJ....163..161T
03260−3558	B 1449BC is a triple in a young (40 Myr) cluster, first 41 yr orbit here.
03284+2248	The subsystem BAG 2Aa,Ab is not detected in 2018-2021, spurious?
03478−1854	This is WDSS 0347502−185407 (TIC 121088959), see 2020ApJS..247...66H
04293−3124	SIG 4 is a brown dwarf. Noisy measures, poor accuracy. Orbit $P = 55$ yr.
04375+1509	CHR 153 contains a subsystem, orbits in 2021AJ....161..144T
04404+1631	CHR 154 is a triple in the Hyades, orbits in 2021AJ....161..144T
05303−6653	A small $\Delta I = -0.06$ mag an does not match $\Delta G = 0.93$ mag, variable?
05321−0305	The resolution of V1311Ori Ba,Bb is reported in 2022AJ....163..127T
05351−0249	A and B components of SKF2259 (Haro 5-2, a PMS star) were resolved into subsystems by Bo Reipurth (2022, in preparation).
06035+1941	MCA 24 is a B8III triple with a 14-day subsystem. The outer orbit is updated here.
06314+0749	Triple system, orbits in 2020AJ....160...69T
07498−0317	This is WDSS 0347502−185407, see 2018MNRAS.480.4884E
08240−1548	HIP 41171 is a quadruple system, see 2019AJ....158..222T
11100−6645	The resolution is reported by Powell et al. 2021AJ....162..299P This is a TESS object with enigmatic eclipses, apparently by dust.
11221−2447	This is a PMS quadrule HD 98800, orbits in 2021A&A...655A..15Z
13175+2024	The subsystem in YSC 129 (HIP 64386) belongs to A, not to B. Preliminary orbits indicate periods of 34 and 5 yr for AB and Aa,Ab, respectively.
15234−5919	B is red, fainter than A in the V band but brighter in I.
16243−5921	The measured pair (0.″99, $\Delta I = 4.2$) is found in Gaia EDR3 at the same position. The parallax is 0.17 mas, so it cannot be the 0.″3 pair HDS2317Aa,Ab
17289−3244	AB (2.″36) is WDSS 1728556−324356, BC is a new pair, see the text.
19250−3205	AB is WDSS 1924594−320432 (TIC 11247221), see 2020ApJS..247...66H; The 0.″08 pair Aa,Ab is new.
21145−7403	This is WDSS 2114277−74024 (HIP 104556), see 2021MNRAS.506.2269E

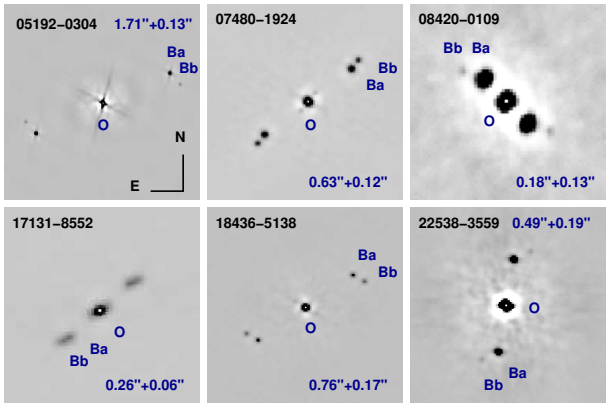

Figure 3. Fragments of speckle ACFs of some newly resolved triple stars. The intensity and spatial scales are chosen for best representation of each system. North is up, east left. Blue letters mark the ACF peaks corresponding to the component's location (as opposed to other symmetric peaks), O marks the ACF center. The outer and inner separations are indicated.

Table 5 *continued*

Table 5 *(continued)*

WDS J2000	Name	ρ (arcsec)	Δm (mag)	Program[a]

Table 5 *(continued)*

WDS J2000	Name	ρ (arcsec)	Δm (mag)	Program[a]
05192−0304	A 53 Ba,Bb	0.37	1.9	MSC[b]
05427−7316	HEI 667 AC	1.35	4.4	NEG
06005−2753	HDS 819 Ba,Bb	0.09	1.6	NEG
06159−5126	RST 179 BC	0.07	1.0	MSC
06223−2021	TDS 3781 BC	0.12	1.4	MSC
07018−1118	HU 112 Ba,Bb	0.04	0.1	MSC[b]
08321−2730	HDS 1220 BC	0.04	0.2	NEG
08420−0109	A 1750 Ba,Bb	0.12	2.7	NEG[b]
08471−4504	TOK 911	0.04	1.0	REF
09046−4104	RSS 189 Aa,Ab	0.06	0.3	HIP[b]
09343−3223	RST 2637 Aa,Ab	0.22	3.3	MSC
10350−5247	B 1685 BC	0.40	2.4	TESS
11247−6139	BSO 5 Aa,Ab	0.25	2.8	MSC
12059+2628	HDS 1707 Ba,Bb	0.07	1.5	HIP

Table 5 *continued*

Table 5 *(continued)*

WDS	Name	ρ	Δm	Program[a]
J2000		(arcsec)	(mag)	
12118−5306	HDS 1722 AB	0.83	5.6	WDS
12282+2502	TOK 912	0.03	0.7	HIP
13514+2620	SKF 260 Ba,Bb	0.25	0.2	MSC[b]
13592−4528	TOK 913	1.20	4.6	REF
17131−8552	JNN 320 Ba,Bb	0.06	0.1	YMG[b]
17289−3244	TOK 914 BC	0.32	2.0	YMG[b]
17373−4300	SEE 510 Aa,Ab	0.24	3.7	WDS
17374−3544	HDS 2488 AC	2.24	5.3	NEG
18153−4928	TOK 915	0.07	0.0	YMG
18248−0621	TOK 320 Ba,Bb	0.13	1.3	MSC
18285−4129	BRT 1058 Aa,Ab	0.17	0.2	YMG[b]
18436−5138	RST 5451 Ba,Bb	0.18	0.3	NEG
18483−3710	JSP 787 Aa,Ab	0.59	3.3	MSC
18581−2953	SKF 1507 Aa,Ab	0.07	1.6	YMG
18581−2953	SKF 1507 Ba,Bb	0.37	0.0	YMG[b]
19250−3205	TOK 916 Aa,Ab	0.08	0.9	YMG
20008−2411	TOK 917	0.70	2.6	HIP
20446−6630	TOK 918	0.08	0.1	HIP
20557−6609	HDS 2981 AC	1.32	6.3	WDS
21433−4327	HDS 3095 Ba,Bb	0.11	3.1	HIP
21510+2911	A 889 Aa,Ab	0.03	0.4	MSC
22039−2451	SEE 465 Aa,Ab	0.65	1.7	MSC[b]
22039−2451	SEE 465 Ba,Bb	0.15	1.9	MSC[b]
22146−2142	TOK 919	0.09	1.1	MSC
22538−3559	HDS 3255 Ba,Bb	0.19	2.1	NEG
23214−1340	HDS 3326 Aa,Ab	0.05	0.0	NEG
23224−5857	TOK 920	0.07	0.1	HIP
23293−5135	TOK 921	0.25	2.7	HIP
23465−4135	TOK 922	0.74	3.4	HIP

[a] HIP – Hipparcos suspected binary; MSC – multiple system; REF – reference star; YMG – young moving groups; NEG – neglected pair; TESS – TESS followup.

[b] See comments in the text.

Table 5 highlights the 50 pairs resolved in 2021 or resolved earlier but not yet published. All measurements of these pairs are found in Table 2. The pairs are identified by the WDS-style codes and the discovery codes or other names. The following columns contain the separation ρ, the magnitude difference Δm, and the observing program. Two pairs were found independently by others, but we keep them in the table for consistency because they are not yet featured in the WDS or its supplement, WDSS. The majority of newly discovered binaries belong to hierarchical systems with three or more components. Typically, new close subsystems in known visual binaries were discovered by HRCam. Comments on some multiple systems are given below, and the speckle ACFs of selected triples are shown in Figure 3.

03385+1336 (HIP 16991, F8) is a quadruple system at 95 pc distance. The outer pair A,B has a separation of 77″, the intermediate pair Aa,Ab (YR 10) is at 0.″27, and the newly discovered subsystem Ab1,Ab2 is at 0.″04. The estimated period of Ab1,Ab2 is ∼10 yr, and it should leave an imprint on the observed motion of Aa,Ab.

05192−0304 (HIP 28419, K3V). The subsystem Ba,Bb in a 1.″5 binary A 53 has been discovered by Hirsch et al. (2021) using adaptive optics. They measured it at 243.°4 and 0.″520 in 2015.410 and determined the magnitude difference of $\Delta K_{\rm Ba,Bb} = 1.2$ mag; another observation was made in 2017.931. Our measurement in 2021 shows that Ba,Bb has retrograde motion and is closing down; its estimated period is 25 yr. The outer pair A,B had a separation of 4.″9 in 1900, and now it closed down to 1.″5. This low-mass triple system is located at 15.7 pc from the Sun.

07018−1118 (HIP 33868, B2V). The main star A is an eclipsing binary GU CMa with a close tertiary companion discovered by eclipse timing. The resolution of Ba,Bb at 0.″04 (AB is at 0.″65) makes this a quintuple hierarchical system. The estimated period of Ba,Bb is 25 yr. More observations are needed to confirm the close pair Ba,Bb and to follow its motion. It cannot be excluded that the eclipsing pair belongs to star B, in which case its tertiary component is identical to Bb and the system is quadruple rather than quintuple.

08420−0109 (HD 74113, A6V) is a strange case. The orbit of the main pair A,B (A 1750) with a period of $P = 250$ yr and a semimajor axis of $a = 0.''205$ is determined here. The new faint star Bb with a separation of 0.″12 from Ba would make the system dynamically unstable, unless its true separation is larger than ∼0.″6. In such case, Bb is an outer companion, and Ba,Bb looks close only in projection. The detection of Ba,Bb is securely confirmed in three observing runs. This subsystem is also apparent in our 2018 observation, although it was overlooked at the time because the ACF was distorted by telescope vibration. Gaia does not give the parallax. The sky is not crowded, making a random superposition of unrelated stars at such close separation extremely unlikely. A similar 0.″48 pair ADS 6941 (BD−00°2045), located at 137″ from AB, also lacks Gaia parallax and PM, and its relation to this triple is presently unknown.

09046−4104 (HIP 44550, G1V) is a three-tier hierarchical system. The inner pair is an eclipsing binary V405 Vel with a 10 day period. It is orbited by star Ab at 0.″06 discovered here with an estimated period of 20 yr. This subsystem explains the large astrometric noise

in Gaia. The outermost component B, at 9.″5 separation, has common PM and parallax.

13514+2620 (HIP 6723, K6V) is a low-mass 2+2 quadruple at 46 pc distance. Aa,Ab is a known 0.″3 pair YSC 50, and Ba,Bb at 0.″25 is discovered here. Both inner pairs have estimated periods of ∼50 yr and large mass ratios. The outer pair A,B at 3.″3 has a period of the order of 1 kyr. Gaia did not measure the parallaxes of A and B because they are close binaries.

17131−8552 (GSC 09526−00895, M0V) is an interesting triple system where the estimated periods of the outer 0.″26 and inner 0.″06 pairs are 25 and 3 yr, respectively. All three stars have comparable magnitudes. Gaia gives no parallax for this star.

17289-3244 (HD 317617, TYC 7379-279-1, K3V). This triple system has been resolved in 2015.41 by Bonavita et al. (2021) in a survey of nearby young stars. They measured BC at 318.°2, 0.″416 with $\Delta H_{\rm BC} = 1.9$ mag.

17373−4300 (HIP 86228, θ Sco, F1III) was observed on request by R. Argyle because it was suspected to be a close pair in Hipparcos. The newly resolved high-contrast 0.″24 pair is different from the known 6.″2 pair SEE 510. The latter in fact is spurious, because it was not seen in the wide-field images taken with HRCam, and the secondary is not found in Gaia. The Hipparcos measurement of this pair at 6.″5 separation is spurious, probably caused by the wrongly interpreted signal from the close pair measured here.

18248−0621 (HIP 90246, K7V) is another nearby (42 pc) 2+2 quadruple system discovered here. The outer binary is at 55″ separation. Its components A and B are revealed to be close pairs with separations of 0.″31 and 0.″13 and estimated periods of 40 yr and 15 yr, respectively. The Gaia astrometry of A and B has large noise owing to their binary nature, but the Gaia parallaxes and PMs of A and B confirm that they form a physical system.

18285−4129 (TYC 7909-2501-1) is a physical triple system. The WDS pair BRT 1058 (5.″2, 178°, $\Delta m = 2$ mag) is not found in Gaia, but a much fainter ($G = 15.48$ mag) Gaia star at 6.″1, 205.°0 from A is a physical companion with common PM and parallax. Star A is resolved here into a 0.″17 pair, although its designation as BRT 1058Aa,Ab appears misleading.

18581−2953 (TYC 6872-1011-1, M0V) is another nearby 2+2 quadruple discovered here by resolving both components of the 28″ pair into 0.″07 and 0.″37 subsystems. The closer one, Aa,Ab, is expected to have a short period of ∼10 yr. The system belongs to a young moving group. Star A was observed at Keck by Ruane et al. (2019), but this close pair was hidden behind the coronagraphic mask of 0.″25 radius, preventing its detection.

22039−2451 (HIP 108923, G6V) contains five components in a hierarchical configuration and is at 57 pc distance from the Sun. The outermost component C is at 122″ from the 3.″4 pair AB (SEE 465 AB). We resolved here both components of SEE 465 into close pairs Aa,Ab (0.″66) and Ba,Bb (0.″15) with estimated periods of 130 yr and 20 yr, respectively, and substantial magnitude differences. Gaia measured matching parallaxes of A, B, and C, while their PMs differ owing to the motion in the inner subsystems. Although Gaia did not resolve Aa,Ab explicitly, it is marked as having double transits, indicating the detection of Ab.

Some wide pairs resolved here are also found in the Gaia EDR3. When parallaxes and PMs of both components are given, the wide pair can be classified as physical (e.g. 13592−4528) or optical (chance projection), as 17374−3544AC.

3.3. *New and Updated Orbits*

Orbits of visual binary stars is a traditional battleground of human ingenuity against inaccurate data and insufficient coverage. Availability of computing power added to various historical methods developed during two centuries such approaches as statistical sampling (e.g. Anguita-Aguero et al. 2022) and a brute-force exploration of the multidimensional parameter space (Blunt et al. 2020). Space astrometry and radial velocities (RVs) are also used nowadays for orbit calculation (Brandt et al. 2021). This field is rejuvenated by recent imaging of substellar and planetary companions and the need to infer their orbits from the short observed arcs. The situation will be further exacerbated by millions of binaries expected in the future data releases of Gaia, e.g. one million binaries published by El-Badry et al. (2021), and lacking coverage of their orbits.

Positional measurements provided by the SOAR speckle program contain a rich material for calculation of new visual orbits and improvement of the known ones. Some orbits resulting from this program are published in (Anguita-Aguero et al. 2022; Gómez et al. 2022; Tokovinin 2021a) and in the circulars of the IAU Commission G1. The quality of these orbits ranges from tentative and preliminary (grades 5 and 4) to good, reliable, and excellent (grades 3 to 1). Orbits are graded using the code and methodology described in ORB6 (Hartkopf, Mason & Worley 2001).

Table 6 lists elements of 174 new and corrected orbits determined from the observations made at SOAR in 2021. The complementary Table 7 contains additional 108 preliminary orbits where no reliable estimates of the

element's errors could be derived. Most preliminary orbits have grades 4 and 5. The constraints on these orbits are insufficient for meaningful estimates of the elements' errors, and some of these orbits will be improved or even dramatically revised in the future as new data are accumulated. Calculation and improvement of orbits is a never ending process where orbital solutions progressively become more reliable and accurate, while new low-grade preliminary orbits are being added to the catalog. Note however that some grade 4 orbits are placed in Table 6 because the errors are well defined. Conversely, some orbits of official grade 3 are still considered preliminary and placed in Table 7. A one-dimensional grading system cannot grasp all aspects of the orbit quality; it is useful for a first-order evaluation. The errors of the elements and the plots provided in the ORB6 catalog give a more comprehensive picture.

Most orbits were fitted by the weighted least-squares method using the IDL program `ORBIT` (Tokovinin 2016c). The weights are proportional to σ^{-2}, and the measurement errors σ are assigned depending on the data source: 2 to 5 mas for speckle interferometry with telescopes of 4 m class and Gaia, 10 mas for Hipparcos, 50 mas and larger for visual micrometer measures. Some outlying visual measures are ignored. We also use the radial velocities where available. Some orbits were fitted using the grid search algorithm (Hartkopf, McAlister & Franz 1989). Different systems of weights are adopted by other orbit computers; usually more weight is given to the historical micrometer data at the expense of a worse fit to the accurate speckle positions.

The orbital elements and their errors (determined by the least-squares fitting) are given in Table 6 in the standard notation. The last columns contain the grade and the reference codes to previously published orbits, when available. The full bibliographic references are provided in the ORB6 online catalog.

Table 6. Visual Orbits with Element's Errors [Fragment]

WDS	Discov.	P	T	e	a	Ω	ω	i	Grade	Ref.[a]
HIP		(yr)	(yr)		(arcsec)	(deg)	(deg)	(deg)		
00219−2300	RST5493 BC	18.441	2019.527	0.831	0.1338	91.3	213.6	92.1	3	Tok2021c
		±0.555	±0.447	±0.034	±0.0204	±1.5	±16.0	±1.7		
00277−1625	YR 1 Aa,Ab	6.586	2014.311	0.762	0.0675	167.2	-0.9	18.5	2	Tok2020e
		±0.027	±0.035	±0.015	±0.0012	±29.9	±31.5	±9.0		
00324+0657	MCA 1 Aa,Ab	27.506	1989.001	0.810	0.1593	105.8	14.3	110.8	2	Jte2018
		±0.051	±0.105	±0.025	±0.0022	±0.8	±2.3	±2.3		
01077−1557	HDS 148	15.493	2019.120	0.980	0.0738	11.0	213.0	66.8	3	Tok2021c
		±0.755	±0.207	fixed	±0.0152	±7.1	±20.3	±11.1		

[a] References to previous orbits are provided in wdsref.txt. Additional references are: Circ204 – Circular of IAU Commission G1, No. 204, 2021; Gomez2022 – Gómez et al. (2022); Horch2021 – Horch et al. (2021);

Table 7. Preliminary Visual Orbits [Fragment]

WDS	Discov.	P	T	e	a	Ω	ω	i	Grade	Ref.[a]
		(yr)	(yr)		(arcsec)	(deg)	(deg)	(deg)		
00258+1025	HDS 57	69.179	2020.847	0.471	0.1413	43.6	59.2	137.0	4	Tok2021c
00304−6236	JNN 296 Aa,Ab	60.644	2016.792	0.664	0.3132	82.1	24.6	130.1	4	first
00348−5853	I 439	350.000	2020.615	0.960	0.7021	119.4	146.2	48.9	4	Tok2021c
01114+1526	BEU 2	62.568	1993.862	0.000	0.4676	120.5	0.0	51.4	4	Tok2021c
01117+0835	HDS 158	47.008	2023.553	0.853	0.1985	132.0	172.6	63.8	4	first

[a] See Notes to Table 6

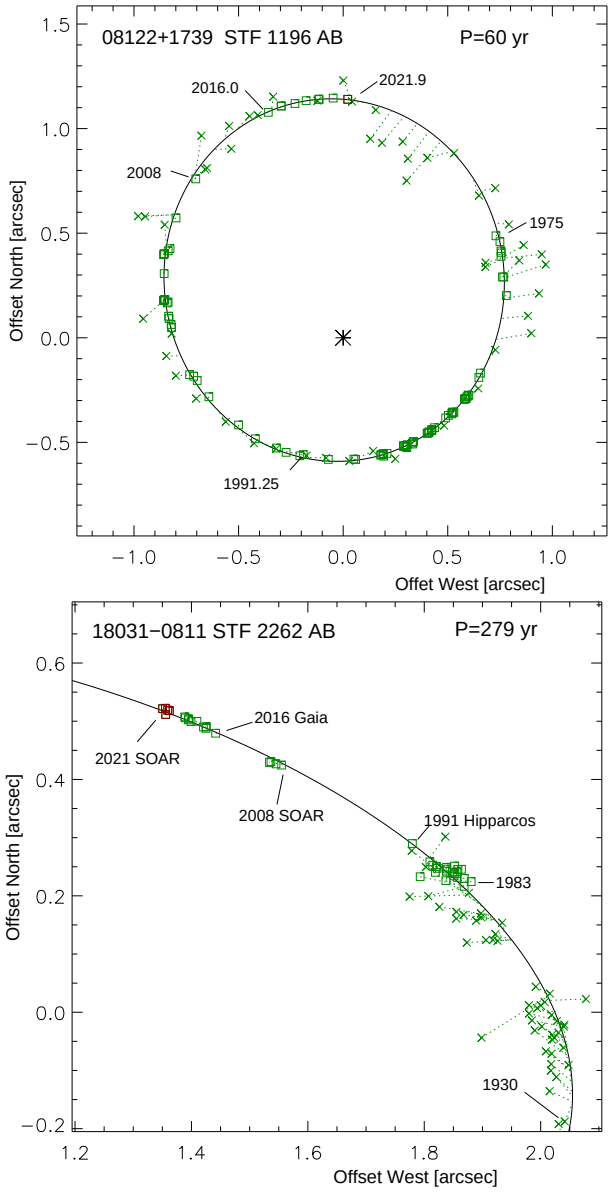

Figure 4. Updated orbits of two calibrators, STF 1196 AB (top) and STF 2262 AB (bottom). Accurate speckle measurements are plotted as squares (red color marks the 2021 observations published here), the less accurate micrometric observations as crosses. Dotted lines connect the positions to the locations on the orbit (ellipse). The scale is in arcseconds, and the main component is at coordinate origin.

Figure 4 shows updated orbits of two calibrator binaries. Although the orbit of STF 1196 (ζ Cnc AB) has been determined many times in the past, its latest update by Izmailov (2019) shows appreciable systematic residuals to the accurate SOAR and Gaia positions. This pair has been measured more than 1000 times since its discovery by W. Struve in 1825, mostly using visual micrometers. However, fitting the orbit to all available data, suitably weighted, does not lead to a good result because the numerous but intrinsically inaccurate visual measurements pull the solution in the wrong direction. Here we use only the micrometer measurements made by W. and O. Struve in the 19th century and ignore all other measurements except speckle interferometry with telescopes of 1.8 m aperture or larger. This pair has been frequently observed by speckle interferometry since 1975 as a calibrator, and the speckle data now cover most of its 60 yr orbit. Our new accurate orbit makes this binary a first class calibrator. It is bright, has a small magnitude difference, and is accessible from both hemispheres. Incidentally, the pair belongs to the nearby (25 pc) quintuple multiple system ζ Cnc, and the orbit of its subsystem Ca,Cb with a period of 17.3 yr is also updated here. With an accurate parallax from future Gaia data releases, both orbits will yield accurate masses.

The bottom panel of Figure 4 shows a more typical calibrator where accurate measurements cover only a small arc of the long-period orbit. The elements fitted with appropriate weights accurately represent this arc. The 18 calibrated SOAR measurements have rms residuals of 3.6 mas and agree very well with the Gaia EDR3 position.

Figure 5 illustrates some orbits determined here for the first time. The bright ($V = 3.0$ mag) star ζ CMa (HIP 30122, HR 2282, 06203−3005) has been resolved at SOAR in 2019.95 and is designated as TOK 821 in the WDS. A spectroscopic orbit with a period of 675 days has been published by Colacevic (1941). Fixing the period to its spectroscopic value, the remaining visual elements are fitted to the 7 measurements made at SOAR so far. Using the Hipparcos parallax of 9.0±0.13 mas, the orbit gives a mass sum of 12.2 $\mathcal{M}_\odot$ for this pair of spectral type B2.5V.

The K5V dwarf HIP 40724 (08187−1512) has been resolved at SOAR in 2018.25 into a binary with a substantial magnitude difference $\Delta I \approx 2.5$ mag. Its orbit with $P = 2.5$ yr uses the unpublished measure in 2016.04 communicated by T. Henry (2021, private communication). The pair passed through the periastron in 2021, and its measurements at close separations are tentative. With the parallax of 28.85±0.56 mas, the orbit corresponds to the mass sum of 1.4 $\mathcal{M}_\odot$. The classical visual binary B 227 (12216−2716, HIP 60281, F5V) was discovered by van den Bos (1928) in 1926. Its 92 yr orbit uses the micrometer measurements (with suitable quadrant adjustment, considering the small Δm), two published speckle-interferometric measurements in the 1980s, and two measurements made at SOAR in 2017 and 2021. Finally, the faint pair of M-type dwarfs CRC 73 (16488+1039) discovered in 2014 by

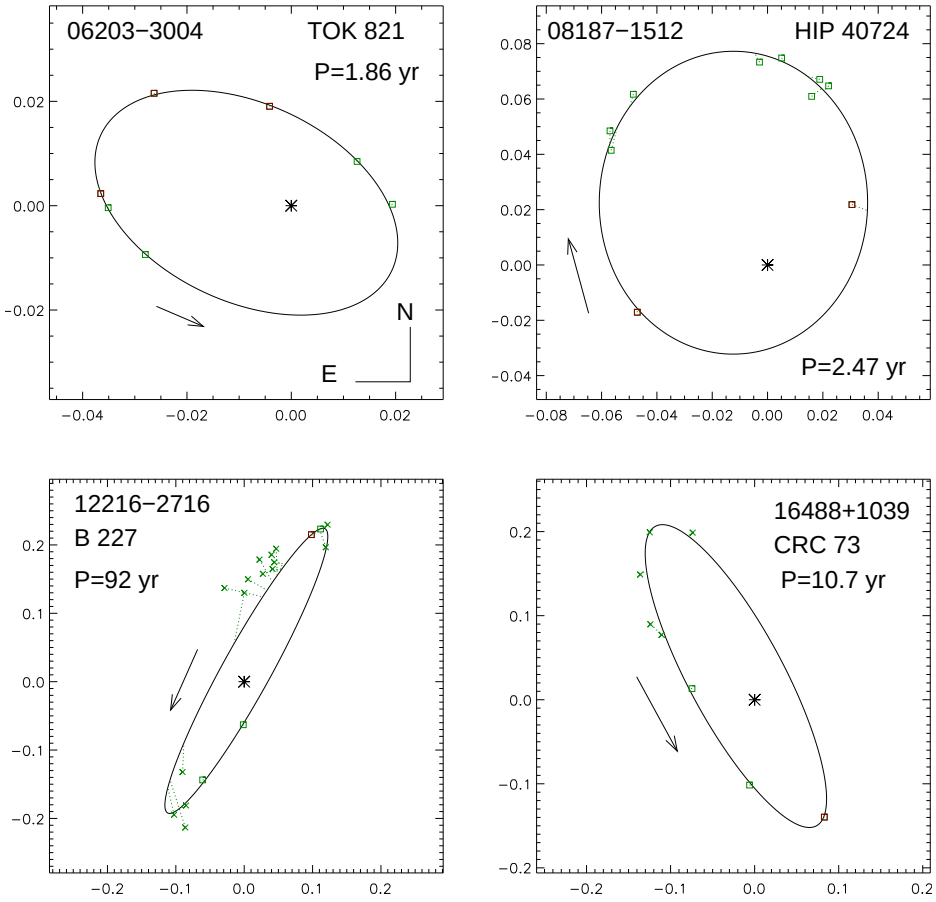

Figure 5. Four orbits computed here for the first time but, nevertheless, relatively well constrained. See the caption to Figure 4.

Cortes-Contreras et al. (2017) and observed at SOAR three times in 2018–2021 has a quasi-circular orbit with $P = 10.7 \pm 1.2$ yr. Despite the grade 4, the orbit is well constrained, and the errors of its elements are modest.

3.4. *Spurious Pairs*

Table 8. Likely Spurious Pairs

WDS	Discoverer	Resolved	Unresolved[a]
00077−5615	HDS 15	0.″1 HIP	2021, L, R
00259−3112	HDS 58	0.″2 HIP	2021, L, R
00292−3755	HDS 65	0.″2 HIP	2021, L, R
00374−3904	WHI 1	0.″3 Sp 1987	2021, R
00386−3903	WHI 2	0.″8 Sp 1987	2021, L, R
00537−7910	HDS 116	0.″1 HIP	2021, L, R
00546−8240	HDS 120	0.″2 HIP	2021, L, R
01475−0753	HDS 240	0.″1 HIP	2021, L, R
01511−7832	HDS 251	0.″2 HIP	2021, L, R
01519−3120	HDS 254	0.″2 HIP	2021, L, R
01571−5031	VOU 20	0.″4 Vis 1929	2021, L, R
02088−6126	HDS 286	0.″1 HIP	2021, R

Table 8 *continued*

Table 8 *(continued)*

WDS	Discoverer	Resolved	Unresolved[a]
02109−7558	HDS 293	0.″3 HIP	2014-21
02376−3659	B 678AB	0.″7 Vis 1927	2021
03023−7154	FIN 360	0.″1 Vis 1961	2021, R
03031−2339	DAM 1296	0.″1 2015	2021
03047−3410	WHI 4	0.″2 Sp 1987	2021, L, R
03096−0100	HDS 405	0.″3 HIP	2021, L, R
04112+1538	CHR 202	0.″1 Sp 1985-86	2018-21, R
04118−2444	DAM 312 Aa,Ab	0.″1	2021, R
04129−1107	HDS 534	0.″2 HIP	2021, L, R
04416−4302	WHI 6	0.″4 Sp 1987	2021
04513−6804	FIN 362	0.″1 Vis 1961	2010-21
04562−0331	HDS 640	0.″2 HIP	2021, L, R
05093−3813	HDS 677	0.″2 HIP	2021, L, R
05343−3626	HDS 737	0.″1 HIP	2021,L, R
05397−0042	BAL 677 Aa,Ab	1.″0 2003	2021, L, R
05488−2507	B 90	0.″2 Vis 1925	2021, R
06113−1635	HDS 844	0.″1 HIP	2021, L
06125−3515	HDS 849	0.″2 HIP	2021, L, R
06226−6238	HDS 872	0.″1 HIP	2021, L, R
06358−1028	HDS 901	0.″2 HIP	2021, R

Table 8 *continued*

Table 8 *(continued)*

WDS	Discoverer	Resolved	Unresolved[a]
06447−3213	PRO 27	1.″1 Vis 1911	2021, L
06596−2754	SEE 73	0.″3 Vis 1897	2021, R
07374−3330	HDS 1079	0.″5 HIP	2021, L, R
08227−1555	HDS 1194	0.″2 HIP	2021, L, R
08542−6142	RST 4901	0.″3 Vis 1942-69	2018-21, L,R
15219−3445	HDS 2162	0.″1 HIP	2021, L, R
15596−5612	HDS 2251	0.″1 HIP	2021, L, R
16015−5416	HDS 2258	0.″2 HIP	2021, L, R
16048−6902	HDS 2271	0.″2 HIP	2021, L, R
16118−5532	HDS 2290	0.″2 HIP	2021, L, R
16243−5921	HDS 2317Aa,Ab	0.″3 HIP	2021, L, R
16398−4706	HDS 2363	0.″1 HIP	2018-21, L, R
17001−1639	HDS 2406	0.″2 HIP	2021, R
17026−5504	HDS 2411 Aa,Ab	0.″2 HIP	2021, L, R
17105−1343	HDS 2425	0.″2 HIP	2021, R
17118−2626	HDS 2429	0.″2 HIP	2021, L, R
17238−2138	HDS 2456	0.″1 HIP	2021, R
17253−5600	HDS 2459	0.″2 HIP	2021, L, R
17254−1643	HDS 2461	0.″2 HIP	2017-21, L, R
17317−0959	HDS 2474	0.″1 HIP	2021, R
17419−0944	HDS 2503	0.″1 HIP	2021, R
17482−2801	HDS 2514	0.″1 HIP	2021, L, R
17492−3315	HDS 2515	0.″2 HIP	2021, L, R
17582−1916	CHR 66	0.″4 Sp 1983	2021, L, R
17583−5010	HDS 2533	0.″2 HIP	2021, L
17587−1152	HDS 2535	0.″1 HIP	2021, R
18052−3921	HDS 2549	0.″3 HIP	2021, L, R
18174−2730	HDS 2585	0.″2 HIP	2021, L, R
18197−4542	CHR 148	0.″3 Sp 1989	2008-21
18218−5526	HDS 2597	0.″1 HIP	2021, L, R
18272+0012	STF2316Aa,Ab	0.″1 vis 1951	2009-21
18320−0607	HDS 2629	0.″1 HIP	2021, L, R
18351−1659	MCA 52	0.″2 Sp 1980	2017-21, L, R
18387−1429	HDS 2641 AB	0.″1 HIP	2014-21
18423−0720	HDS 2649	0.″1 HIP	2008-21, R
18501−0823	HDS 2670	0.″1 HIP	2013-21, L, R
19020−1705	OCC 9061	0.″1 Occ 2014	2021, R
19024−2541	HDS 2699	0.″2 HIP	2021, R
19044−0541	HDS 2704	0.″2 HIP	2021, R
19205−0525	ISO 10 Aa,Ab	0.″5 Sp 1987	2021
19223−2226	I 1399	0.″4 Vis 1925	2021
19230−0144	HDS 2743	0.″1 HIP	2021, L, R
19293−6833	HDS 2769	0.″2 HIP	2021, L, R
19317−3153	VOU 85	0.″1 Vis 1937	2021, L, R
19383−1527	ARU 16	0.″7 Sp 1984	2021, L, R
19420−2223	HDS 2793	0.″1 HIP	2021, L, R
19425−1607	BU 1288	0.″2 Vis 1889	2021, R
19460−0735	HDS 2808	0.″1 HIP	2021, L, R
19492+0817	ARU 17	0.″4 Sp 1984	2021, R
20007−1757	ARU 18	0.″4 Sp 1984	2021, L, R
20020−1754	ARU 19	0.″4 Sp 1984	2021, L, R
20029−8455	HDS 2859	0.″2 HIP	2021, L, R
20109−0637	ARU 20	0.″5 Sp 1984	2021, L, R
21104−4114	ARU 3	0.″2 Sp 1984	2021, R

Table 8 *continued*

Table 8 *(continued)*

WDS	Discoverer	Resolved	Unresolved[a]
21415−7723	BLM 6	0.″1 Sp 1976	2021
21420−2940	HDS 3090	0.″1 HIP	2021, L, R
22456−8529	JSP 836	0.″7 Vis 1929	2021, R
22461−1210	ARU 5	0.″3 Sp 1982	2014-21
22473−3410	CHR 189 AB	0.″3 Sp 1992	2015-21, R
22532−1102	HDS 3249	0.″2 HIP	2021, L, R
23114−4259	B 594	0.″2 vis 1925-63	2008-21
23256−2556	HDS 3332	0.″2 HIP	2021, L, R

[a] Additional indications of the spurious nature of visual pairs: R – no excess noise in Gaia EDR3, RUWE<2; L – long estimated period;

In 2021, we observed a substantial number of "neglected" pairs that have only one documented resolution and no further confirming observations. Our measurements provide such confirmation and in several cases reveal additional close subsystems (section 3.2). Some pairs were not resolved because orbital motion decreased their separation below the detection limit of HRCam. Such binaries are candidates for future observations and, eventually, orbit calculation. However, the majority of unresolved double stars are spurious discoveries. A list of spurious pairs was presented in (Tokovinin et al. 2019); here we continue this effort and list another 94 apparently spurious pairs in Table 8. Its columns contain WDS code, discoverer designation, separation in arcseconds, observing method (HIP — Hipparcos, Sp — speckle interferometry, Vis — visual micrometer, Occ — occultation), and years when the pair was resolved. The last column gives the years when the pair was not resolved at SOAR (some targets have multiple observations) and additional indications from Gaia that the star is single, explained below. Pairs in Table 8 have an 'X' code added to their entry in the WDS, indicating the pair is not real.

Gaia EDR3 does not contain measurements of close double stars, but gives several clues concerning their reality. Pairs with separations from 0.″15 to 0.″7 and modest magnitude difference have no parallaxes and PMs in EDR3. Gaia astrometric solutions with excessive noise caused by companions are distinguished by the reduced unit weight error (RUWE) parameter, which is less than 1.4 for point sources and can be larger for binaries. Furthermore, the Gaia parallaxes allow us to evaluate orbital periods from projected separations. Take for example the first entry in Table 8, 00077−5615 (HDS 15). Hipparcos measured in 1991.25 a separation of 0.″142 that corresponds to 153 au, given the parallax of 0.93 mas from Gaia EDR3. The orbital semimajor axis cannot be less than half of the separation, so the

minimum period computed by the third Kepler's law is 481 yr (assuming a mass sum of 2 $\mathcal{M}_\odot$). The real period is likely longer, so the hypothesis that this pair has closed down in 30 yr between the Hipparcos and SOAR observations cannot be true. HDS 15 is thus definitely spurious, and RUWE=1.0 confirms this. The letters L (long-period) and R (small RUWE) in the last column of Table 8 mark similar cases. An opposite example is 11557−1438 (RST 3761). This pair has been consistently unresolved at SOAR between 2018 and 2021. However, it was measured several times between 1937 and 1989, has a RUWE=2.3, and the parallax of 4.5 mas suggests an orbital period on the order of 200 yr. So, RST 3761 is a real binary, it just closed down at present. In our future work, we will check neglected pairs using Gaia to avoid wasting telescope time for their observation.

Most entries in Table 8 are Hipparcos pairs with separations of 0.″2 or less. This is below the diffraction limit of the 30 cm Hipparcos aperture. The majority of Hipparcos pairs with comparable separations are real, and a small number of spurious resolutions could be caused by problems in the data reduction. Spurious binaries discovered by visual observers and never confirmed are also found in our list. The third group of spurious pairs results from speckle interferometry. Several false discoveries have been made by HRCam and later retracted (see Tokovinin et al. 2019). The discovery codes ARU (Argue et al. 1985), WHI (White et al. 1991), and ISO (Isobe 1991) correspond to early speckle programs that produced a number spurious pairs owing to lack of experience with this technique.

4. SUMMARY AND OUTLOOK

The total number of observations made with HRCam to date is about 30,300. This paper documents the observations made in 2021 and their use for improving the orbits. It reports 50 newly resolved pairs (the majority of which are members of triple and higher-order systems) and gives a list of likely spurious pairs checked at SOAR.

Speckle interferometry was invented half a century ago and now it has completely replaced the visual micrometer measurements. The time span of speckle data becomes comparable to the 100–200 yr of visual coverage, and in some cases the latter loses its scientific value, as illustrated by the first orbit in Figure 4. Furthermore, the historic visual double stars, still a majority of the WDS entries, are complemented by the new Hipparcos and speckle pairs. Millions of Gaia pairs will soon completely dominate over the present-day sample of double stars. So, will the current speckle programs be viable in the future, or will they progressively lose their importance, retaining only a historic value, like the visual micrometer measurements or the Ptolemeus astrometric catalog? We believe that in the near term, the demand for new speckle data will actually increase, being driven by Gaia and other missions.

The Gaia catalog already contains accurate relative positions, motions, and parallaxes of many thousands of double stars wider than ∼0.″7 and gives hints on the closer pairs (missing parallaxes or a large RUWE). Accurate parallaxes add value to the visual orbits, enabling good measurement of stellar masses. Although the current Gaia parallaxes of visual binaries are often biased by orbital motion, this caveat will be corrected in the next data release 3 which will account for acceleration. Unbiased parallaxes of single components in visual triples, available now in the EDR3, can also serve for the mass measurent of their inner orbital pairs.

The huge future impact of Gaia on the binary star research can be gleaned by looking back at the Hipparcos mission, which revealed thousands of close pairs missed by the historic visual surveys. Follow-up speckle monitoring of the Hipparcos binaries (including the work reported here) leads to the determination of their orbits and masses. The Gaia binaries will require a similar follow-up, but their large number will necessitate a selective strategy. Determination of all potentially accessible orbits (the default approach until now) will be replaced by the astrophysically motivated samples. Obvious candidates are low-mass nearby stars (see e.g. Vrijmoet et al. 2022), high-mass stars, pre-main-sequence stars, binaries hosting exoplanets, and hierarchical systems. So, the demand for new observations of close visual binaries will likely increase in the near future.

We are grateful to the anonymous referee for a thorough check of the data. We thank the SOAR operators for efficient support of this program, and the SOAR director J. Elias for allocating some technical time. This work is based in part on observations carried out under CNTAC programs CN2019A-2, CN2019B-13, CN2020A-19, CN2020B-10, and CN2021B-17. R.A.M. and E.C. acknowledge support from the FONDECYT/CONICYT grant No. 1190038. The research of A.T. is supported by the NSFs NOIRLab.

This work used the SIMBAD service operated by Centre des Données Stellaires (Strasbourg, France), bibliographic references from the Astrophysics Data System maintained by SAO/NASA, and the Washington Double Star Catalog maintained at USNO. This work has made use of data from the European Space Agency (ESA) mission Gaia (https://www.cosmos.esa.int/gaia) processed by the Gaia Data Processing and Analysis Consortium (DPAC, https://www.cosmos.esa.int/web/gaia/dpac/consortium). Funding for the DPAC has been provided by national institutions, in particular the institutions participating in the Gaia Multilateral Agreement.

Facility: SOAR.

REFERENCES

Anguita-Aguero, J., Mendez, R., Claveria, R. M., & Costa, E. 2022, AJ, 163, 118

Argue, A.N., Hebden, J. C., Morgan, B. L. et al. 1985, MNRAS, 216, 447

Blunt, S., Wang, J., Angelo, I., et al. 2020, AJ, 159, 89

Bonavita, M., Gratton, R., Desidera, S. et al. 2021, ArXiv preprint 2103.13706

Brandt, T. D. 2021, ApJS, 254, 42

Brandt, T. D., Dupuy, T. J., Li, Y., et al. 2021, AJ, 162, 186

Colacevic, A., 1941, Oss. e Mem. Arcetri 59, 15

Cortes-Contreras, M., Bejar, V. J. S., Caballero, J. A., et al. 2017, A&A, 597, 47

El-Badry, K., Rix, H.-W., & Heintz, T. M. 2021, MNRAS, 506, 2269

Gaia Collaboration, Brown, A. G. A., Vallenari, A., et al. 2021, A&A, 649, A1 (Gaia EDR3)

Gómez, J., Docobo, J. A., Campo, P., Andrade, M., Mendez, R., & Costa, E. 2022, MNRAS, 509, 4229

Hartkopf, W. I., Mcalister, H. A., & Franz, O. G. 1989, AJ, 98, 1014

Hartkopf, W. I., Mason, B. D. & Worley, C. E. 2001, AJ, 122, 3472 (ORB6)

Hartkopf, W. I., Tokovinin, A. & Mason, B. D. 2012, AJ, 143, 42

Hirsch, L. A., Rosenthal, L., Fulton, B. J., et al. 2021, AJ, 161, 134

Horch, E. P., van Belle, G. T., Davidson, J. W., Jr., et al. 2015, AJ, 150, 151

Horch, E. P., Casetti-Dinescu, D. I., Camarata, M. A., et al. 2017, AJ, 153, 212

Horch, E. I., Tokovinin, A., Weiss, S. A., et al. 2019, AJ, 157, 56

Horch, E. P., Broderick, K. G., Casetti-Dinescu, D. I., et al. 2021, AJ, 161, 295

Isobe, S. Proc. Astron. Soc. Australia, 1991, 9, 270

Izmailov, I. S. 2019, AstL, 45, 30

Kenyon, S., Lawrence, J. S., Ashley, M., et al. 2006, PASP, 118, 924

Mason, B. D., Wycoff, G. L., Hartkopf, W. I., et al. 2001, AJ, 122, 3466 (WDS)

Mendez, R. A., Clavería, R. M., Orchard, M. E., & Silva, J. F. 2017, AJ, 154, 187

Ruane, G., Ngo, H., Mawet, D. et al. 2019, AJ, 157, 118
Tokovinin, A. 2012, AJ, 144, 56
—. 2016b, Orbit: IDL Software For Visual, Spectroscopic, And Combined Orbits, Zenodo, doi: 10.5281/zenodo.61119
Tokovinin, A. 2018, PASP, 130, 5002
Tokovinin, A. 2021a, AJ, 161, 144
Tokovinin, A. 2021b, Universe, 7(9), 352
Tokovinin, A. 2022, AJ, 163, 127
Tokovinin, A. & Briceño, C. 2020, AJ, 159, 15
Tokovinin, A. Cantarutti, R., Tighe, R., et al. 2010b, PASP, 122, 1483
Tokovinin, A. & Latham, D. W. 2020, AJ, 160, 251
Tokovinin, A., Mason, B. D., & Hartkopf, W. I. 2010a, AJ, 139, 743 (TMH10)
Tokovinin, A., Mason, B. D., & Hartkopf, W. I. 2014, AJ, 147, 123
Tokovinin, A., Mason, B. D., Hartkopf, W. I., et al. 2015, AJ, 150, 50
Tokovinin, A., Mason, B. D., Hartkopf, W. I., et al. 2016, AJ, 152, 116
Tokovinin, A., Mason, B. D., Hartkopf, W. I., et al. 2018, AJ, 155, 235
Tokovinin, A., Mason, B. D., Mendez, R. A., et al. 2019, AJ, 158, 148
Tokovinin, A., Mason, B. D., Mendez, R. A., et al. 2020, AJ, 160, 7
Tokovinin, A., Mason, B. D., Mendez, R. A., Costa, E., Mann, A. W., & Henry, T. J. 2021, AJ, 162, 41
van den Bos, W. H. 1928, Ann. Leiden Obs. 14, Pt.4
Vrijmoet, E. H., Tokovinin, A., Henry, T. J., et al. 2022, AJ, 163, 178
White, G. L., Jauncey, D. L., Reynolds, J. E. et al. 1991, MNRAS, 248, 411
Ziegler, C., Tokovinin, A., Briceño, C., et al. 2020, AJ, 159, 19
Ziegler, C., Tokovinin, A., Latiolais, M., Briceño, C., Law, N., & Mann, A. W. 2021, AJ, 162, 192